AD-A125 055 PHYSICAL CONSTANTS FOR MICROWAVE DISCHARGE(U) SRI INTERNATIONAL MENLO PARK CA S A DAMRON ET AL. 16 SEP 82 N00019-81-C-0479 1/1

UNCLASSIFIED F/G 20/3 NL

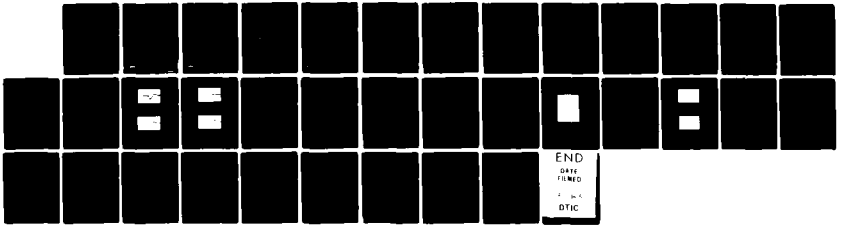

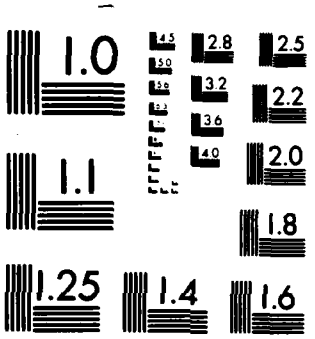

MICROCOPY RESOLUTION TEST CHART
NATIONAL BUREAU OF STANDARDS-1963-A

Final Report *October 1982*

AD A125055

PHYSICAL CONSTANTS FOR MICROWAVE DISCHARGE

By: S. A. DAMRON G. AUGUST

Prepared for:

NAVAL AIR SYSTEMS COMMAND
DEPARTMENT OF THE NAVY
WASHINGTON, D.C. 20361
Attention: JAMES WILLIS, CODE 310B

CONTRACT N00019-81-C-0479

SRI Project 3681

MAR 1 1983

A

DISTRIBUTION LIMITED TO U.S. GOVERNMENT AGENCIES ONLY;
[illegible]
DATE;
OTHER REQUESTS FOR THIS DOCUMENT
MUST BE REFERRED TO COMMANDER,
NAVAL AIR SYSTEMS COMMAND, AIR-

DTIC FILE COPY

SRI International
333 Ravenswood Avenue
Menlo Park, California 94025
(415) 326-6200
Cable: SRI INTL MPK
TWX: 910-373-2046

APPROVED FOR PUBLIC RELEASE:
DISTRIBUTION UNLIMITED

83 1 031

SRI International

Final Report *October 1982*

PHYSICAL CONSTANTS FOR MICROWAVE DISCHARGE

By: S. A. DAMRON G. AUGUST

Prepared for:

NAVAL AIR SYSTEMS COMMAND
DEPARTMENT OF THE NAVY
WASHINGTON, D.C. 20361
Attention: JAMES WILLIS, CODE 310B

CONTRACT N00019-81-C-0479

SRI Project 3681

Approved by:

JOHN B. CHOWN, *Director*
Electromagnetic Sciences Laboratory

DAVID A. JOHNSON, *Vice President*
System Technology Division

DISTRIBUTION LIMITED TO U.S. GOVERNMENT AGENCIES ONLY;
☐ FOREIGN INFORMATION
☐ PROPRIETARY INFORMATION
☐ TEST AND EVALUATION
☐ CONTRACTOR PERFORMANCE EVALUATION
DATE:
OTHER REQUESTS FOR THIS DOCUMENT MUST BE REFERRED TO COMMANDER, NAVAL AIR SYSTEMS COMMAND, AIR-

APPROVED FOR PUBLIC RELEASE:
DISTRIBUTION UNLIMITED

SRI INTERNATIONAL, 333 Ravenswood Avenue, Menlo Park, California 94025
(415) 326-6200, Cable: SRI INTL MPK, TWX: 910-373-2046

UNCLASSIFIED

SECURITY CLASSIFICATION OF THIS PAGE (When Data Entered)

REPORT DOCUMENTATION PAGE

READ INSTRUCTIONS BEFORE COMPLETING FORM

1. REPORT NUMBER

2. GOVT ACCESSION NO. A125055

3. RECIPIENT'S CATALOG NUMBER

4. TITLE (and Subtitle)

Physical Constants For Microwave Discharge

5. TYPE OF REPORT & PERIOD COVERED

Final Report
17 Sept 1981 - 16 Sept 1982

6. PERFORMING ORG. REPORT NUMBER

SRI Project 3681

7. AUTHOR(s)

S. A. Damron, G. August

8. CONTRACT OR GRANT NUMBER(s)

N00019-81-C-0479

9. PERFORMING ORGANIZATION NAME AND ADDRESS

SRI International
333 Ravenswood Avenue
Menlo Park, California 94025

10. PROGRAM ELEMENT, PROJECT, TASK AREA & WORK UNIT NUMBERS

11. CONTROLLING OFFICE NAME AND ADDRESS

Department of the Navy
Naval Air Systems Command
Washington, D.C. 20361 Attn: Code AIR-310

12. REPORT DATE
16 Sept 1982

13. NO. OF PAGES
(25)

14. MONITORING AGENCY NAME & ADDRESS (if different from Controlling Office)

15. SECURITY CLASS. (of this report)

15a. DECLASSIFICATION/DOWNGRADING SCHEDULE

16. DISTRIBUTION STATEMENT (of this report)

Unlimited Distribution

APPROVED FOR PUBLIC RELEASE:
DISTRIBUTION UNLIMITED

DISTRIBUTION LIMITATION
DATE:
OTHER REQUESTS FOR THIS DOCUMENT
MUST BE REFERRED TO COMMANDER,
NAVAL AIR SYSTEMS COMMAND, AIR-

APPROVED FOR PUBLIC RELEASE:
DISTRIBUTION UNLIMITED

17. DISTRIBUTION STATEMENT (of the abstract entered in Block 20, if different from report)

18. SUPPLEMENTARY NOTES

The views, opinions, and/or findings contained in this report are those of the authors and should not be construed as an official Department of the Navy position, policy, or decision unless so designated by other official documentation.

19. KEY WORDS (Continue on reverse side if necessary and identify by block number)

MICROWAVE DISCHARGE, MICROWAVE PLASMA, PLASMA CHARACTERISTICS

20. ABSTRACT (Continue on reverse side if necessary and identify by block number)

Physical characteristics of gas breakdown caused by high-powered microwaves were studied experimentally. Since conditions for initiating breakdown have been studied theoretically and experimentally, this study concentrated on characterizing the breakdown plasma. The characteristics measured were plasma size, strength of the pressure wave emanating from the discharge, and the ion current collected on an electrostatic probe inserted in the plasma. From these measurements it was possible to estimate the temperature of the plasma, the efficiency of the plasma as a microwave absorber, and the electron and ion densities in the plasma.

DD FORM 1 JAN 73 1473

EDITION OF 1 NOV 65 IS OBSOLETE

UNCLASSIFIED

SECURITY CLASSIFICATION OF THIS PAGE (When Data Entered)

19. KEY WORDS (Continued)

20 ABSTRACT (Continued)

The experiments were made at the SRI microwave facility, which uses a 250 kW X-band (9.375 GHz) transmitter for its microwave source. The microwave energy is focused into a vacuum vessel (a bell jar) using a horn feed and a parabolic reflector. In the vacuum vessel a reflecting plate serves both to focus the microwave energy above the plate and as a mount for instrumentation that measures the discharge region.

Camera measurements of the discharge showed that the discharge regions formed in the antinodal regions above the reflecting plate and took the shape of small pancakes. The lowermost and largest discharge region was about 2 cm in diameter and 2 mm thick. It floated about 8.7 mm above the reflecting plate, so that its distance from midplasma to reflecting plate was 9.7 mm. This was slightly higher than the 8 mm calculated as the antinodal point of the 9.735 GHz wave.

A pressure transducer was mounted in the reflecting plate directly beneath the center of the plasma above it. The Mach numbers of the pressure waves emanating from the discharge region ranged from 1, when no breakdown occurred (this happened at higher ambient pressures), to a maximum of between 1.33 and 1.44.

From the camera and the pressure transducer measurements, it was possible to calculate theoretically the maximum temperature in the plasma. This was calculated to be between 838 and 1061°K. It also possible to estimate the microwave absorption efficiency of the plasma. The flux to the discharge region was measured as 1.62 kW/cm^2. The internal energy per molecule can be determined for the case where all power flux is absorbed and for the case where the plasma reaches the range of temperature it reached. The ratio of these internal energies gives the absorption efficiency of the plasma, which is between 64 and 90%. Despite the uncertainity in the measurement, the absorption efficiency of the plasma is very high.

Single-probe measurements in the middle of the plasma were made to monitor ion current throughout the discharge. The peak ion and electron denisties were estimated two ways. In the first way, the densities were determined from free molecular and continuum theory using the actual peak current measured. The ion density, and by implication the electron density, was estimated as $5.9 \times 10^{12}/cm^3$. In the second way, free molecular theory was used to calculate the ion density from the ion current 1 μs after the end of the breakdown. This density value was extrapolated back to the peak value. Since the peak density occurred in a slightly nonfree molecular environment, and the density 1 μs after the breakdown occurred in a free molecular environment, this second approach probably yielded a more accurate lower bound to the actual ion and electron densities. The extrapolated ion and electron densities were $6.9 \times 10^{12}/cm^3$.

CONTENTS

Accession For
NTIS GRA&I
DTIC TAB
Unannounced
Justification
By
Distribution/
Availability Codes
Dist | Avail and/or Special
A

DTIC COPY INSPECTED 2

ILLUSTRATIONS

ACKNOWLEDGMENTS

The authors would like to express their thanks to the technical staff at SRI, especially Robert Mora and Ted Swift. Mr. Swift spent many hours fine-tuning the microwave apparatus and making experimental runs. Thanks also to Rebecca Moseley for her help preparing the quarterly and final reports. We would like to thank James Willis of the Naval Air Systems Command for his help. Mr. Willis provided focus and direction to the project and helped coordinate our work with other scientists studying similar microwave phenomena.

I INTRODUCTION

Highly concentrated microwave energy acting on a gas can produce a plasma of electrons and ions known as a gas discharge, or breakdown. A discharge region modifies the normal transmission of microwaves through gas. The discharge plasma reflects some of the incident microwave energy, and the energy absorbed by the plasma is reradiated in a variety of mechanical and electromagnetic forms. Studies of possible applications of high-power microwaves require some knowledge of self-induced discharge plasmas, since the discharge limits the delivered energy. The Navy, as well as other DoD agencies, has examined potential military applications of high-power microwave radiation.[1*] Some postulated uses involve straight-forward use of high-power sources to replace existing low-power sources in radar, jamming, or communications systems, thereby achieving greater range capability, interference, and signal level. Other postulated applications use the strong fields, high powers, or large energies to obtain unique or unusual effects, such as damage, blinding, and disruption of radar beams. While some applications are limited by air breakdown, several other uses depend on air breakdown for their effectiveness.

The threshold conditions for microwave breakdown of air are fairly well understood theoretically and have been substantially verified experimentally.[2,3] This report presents the results of a study that concentrated on the physical characterization of the plasma itself. Several experiments were performed, including measurements of the physical dimensions of the breakdown region, the strength of the pressure wave emanating from the breakdown, the light flux from the

---

* References are listed at the end of this report.

breakdown, and the ion current collected by probes inserted in the plasma.

The experiments described in this report establish some data points for use in testing current theories on microwave discharges. The theories, which are being developed by the Naval Research Laboratory and by various contractors to the Navy, relate several breakdown parameters, such as size and incident microwave power flux, to plasma heating.[4] Of the five experiments conducted, four were used in the analysis. Plasma size and discharge pressure were measured to calculate the plasma heating. The microwave power flux to the discharge region was also measured and, in conjuction with the heating results, was used to calculate the plasma's absorption efficiency. Ion current was measured using Langmuir probes to determine the density of ions and electrons in the plasma. The optical output of plasma discharge was also measured in conjunction with the plasma size measurements. Section III describes the actual experiments in detail; Section IV presents the results deduced from the data.

As in any experimentation on systems as complicated as a gas discharge, much of the interpretation of the raw data depends on theories relating the response of various sensors to the physical phenomenon at hand. Nevertheless, the raw data presented here increase the knowledge of microwave discharges, and the interpreted data provide some initial points for use in discharge theories.

II SRI MICROWAVE FACILITY

The SRI Microwave Facility (Figure 1) contains a high-power transmitter capable of emitting a 250 kW, 8 μs (or shorter) RF pulse, at X-band (9.375 GHz). The transmitter can operate at a rate of a few pps up to a repetition rate limited by the maximum allowable duty cycle (0.001). The transmitter is focused into a vacuum vessel (bell jar with plastic cover) via a horn feed and a parabolic dish antenna. The 3 dB width of the focal region, transverse to the beam propagation direction, is 1.4 wavelengths. Microwave absorber material surrounds the bell jar on the outside and lines the bottom (inside) to minimize reflections. A metal reflecting plate can be placed inside the bell jar at the focal plane to produce standing waves of electric fields. The power level and system efficiency allow breakdown to occur at pressures up to 20 torr without a reflecting plate, and up to about 35 torr with a reflecting plate. The ratio of the collision frequency to radian radio frequency at those pressures ranges from 2 to 3 times. This is just adequate to produce some desired collision-dominated effects.[5]

Each measurement required slight modifications to the facility. These modifications will be described in conjuction with each experiment.

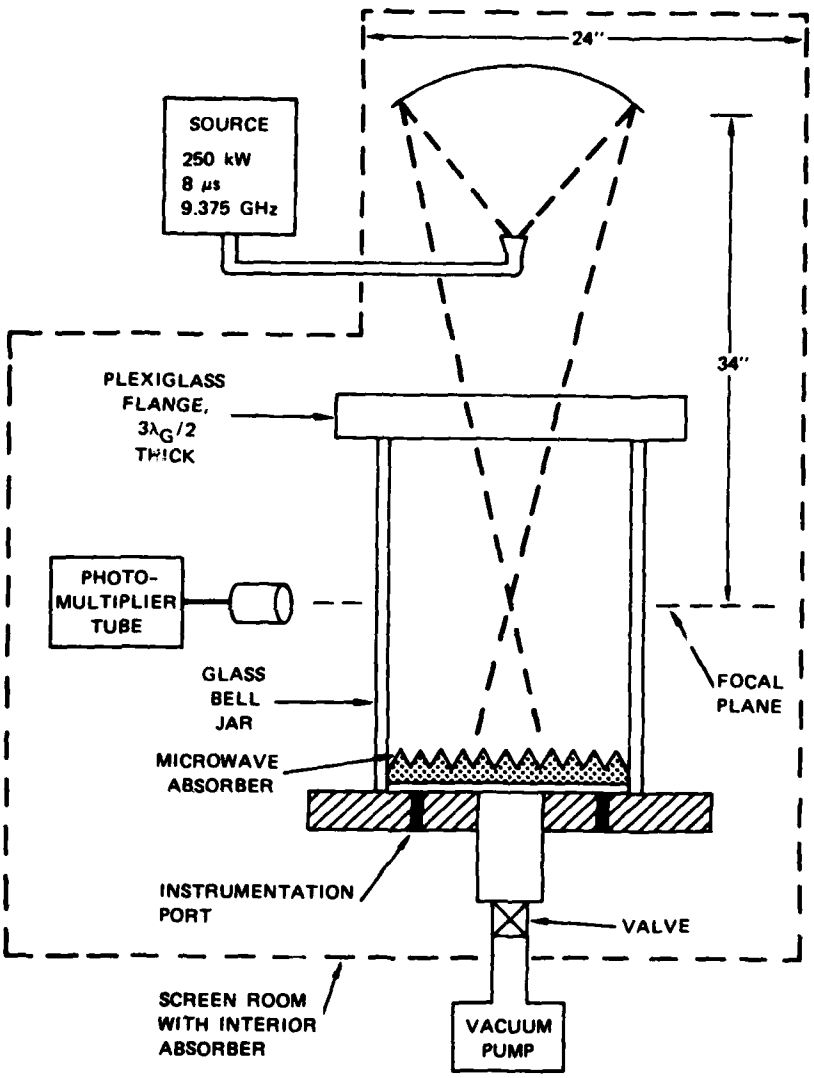

FIGURE 1 SRI MICROWAVE FACILITY TEST ARRANGEMENT

III EXPERIMENTS

A. Dimensions of the Discharge Plasma Region

The microwave feedhorn was adjusted to increase the microwave power focused on the discharge region. After this adjustment, photographs of the plasma were taken with the reflecting plate in place to determine the plasma dimensions. A camera was mounted outside the jar as close to the height of the plasma as possible, first with the film plane parallel to the E-field lines, and then with the film parallel to the H-field lines. Two rules were attached to opposite sides of the vacuum vessel, one as close as possible to the camera, the other as far as possible from the camera. The rules allowed for parallax and scale correction in each photograph.

The discharge regions looked like small-diameter, floating pancakes, parallel with, and evenly spaced in, the antinodal regions above the reflecting plate. The number of discharge regions increased when the microwave power was increased or when the ambient pressure in the vacuum vessel was decreased. At very low pressures (< 20 torr), the discharge plasmas became less defined and spread up and down between the antinodal discharge regions. The photographs used to calculate the plasma dimensions were exposed to between 10 and 100 RF pulses, each 8 μs long.

The lowermost and largest plasma was 1.9 mm (±0.1 mm) thick. At 30 torr ambient pressure, the width of plasma when the film plane was parallel to the E-field lines was 2.0 cm, and 1.2 cm when the film plane was parallel to the H-field lines. Both these widths are much less than the 3 dB width of the microwave focal region beam. The measurements of discharge thickness and width were used in calculating the theoretical heating of the plasma (see Section IV-A).

The visible bottom of the lowermost plasma was 8.7 mm above the reflecting plate. This put the center of the plasma at about 9.7 mm above the reflecting plate. This result was higher than anticipated, since the first antinodal region of the 9.375 GHz radiation was predicted to be at 8.0 cm. The higher 9.7 mm result was later used in calculating the travel distance of shock waves emanating from the discharge (see Section III-B).

B. Pressure Pulses Emanating from Discharges

Heating in the plasma was determined indirectly by measuring the pressure pulses emanating from a microwave discharge. The experimental set-up was modified by mounting a pressure transducer in the reflecting plate underneath the discharge regions. A thick reflecting plate was used in this experiment to increase the inertia of the plate and reduce its response to the shock waves. The pressure transducer, a Kistler model 603A, was mounted 1 cm from the center of the plate, which was as close as possible to the center of the microwave discharge region above it. The Kistler transducer has the following characteristics:

- Frequency response — 400 kHz
- Rise time — 1 μs
- Pressure range, full scale — Up to 3000 psi
- Resolution — 0.05 psi
- Sensitivity (nominal) — 0.35 pCb/psi.

A charge amplifier provided by Kistler for this transducer was initially included in the set-up, but its electronic noise dominated the low-level discharge signals. The Kistler amplifier was replaced with a Princeton Applied Research model 113 preamplifier, which matched the impedance of the transducer and had a high-frequency roll-off of 300 kHz.

Initial calibrations assumed a linear transducer response over the transducer's operating range. Since this assumption proved incorrect over the range of pressures apparently being measured, R. Blomenkamp of SRI's Poulter Laboratory suggested a deadweight calibration, in which small weights are suddenly removed from the surface of the transducer. The transducer response via the preamplifier can then be compared to the

ratio of the applied weight to the area of the transducer. The procedure yielded a calibration of 0.9 torr per millivolt (±20%) of preamplifier response with the preamplifier gain at 100. The high uncertainty was due to the introduction of mechanical energy (slipping and sliding) to the transducer as the weight was removed from the transducer's diaphragm. Another uncertainity in the transducer calibration resulted from the difference between the transducer's response in the calibration frequency range, about 200 Hz, and in the range of the pressure pulse response, about 300 kHz. The 0.9 torr-per-millivolt response is the value used for interpretting the data presented here. As mentioned in Section III-A, the experimental arrangement produced a discharge region with a 2 cm diameter and 0.19 cm thickness, floating about 1 cm above the reflecting plate. The pressure wave emanating from the discharge region can be treated approximately as a one-dimensional shock.

The output from the Princeton Applied Research preamplifier was recorded on an oscilloscope, and the resulting experimental traces are shown in Figures 2 through 5. These oscillograms always contain two traces. The top trace shows the RF power that generates the discharge regions. This trace is inverted in that when the microwave power is on, the trace is low (at the beginning of the trace), and when the power is off, the trace is high. The bottom trace shows several time histories of pressure pulses arriving at the reflecting plate. Note that the RF power causes a spurious transducer response. This response decays quickly enough, however, that the pressure pulse is recorded without any residual spurious signal. Each oscillogram shows several discharges at the same microwave power level and ambient pressure. The pulse repetition rate, driven by an external trigger, was 10 pps for this case and each pulse was 4 μs long. The oscillograms show that the general time histories of the pressure waves are similar, but that the amplitudes change substantially from pulse to pulse. Some of the traces are flat during the period in which a pressure pulse would be expected. This indicates that occasionally no discharge occurred during the RF pulse (this only happened at high pressures, when the peak

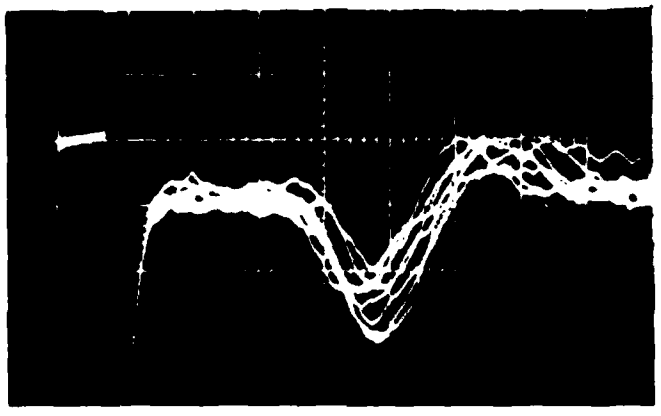

FIGURE 2 PRESSURE PULSE AT 16 torr AMBIENT PRESSURE
(100 preamplifier gain, 4-μs RF pulse, 8 discharge regions)

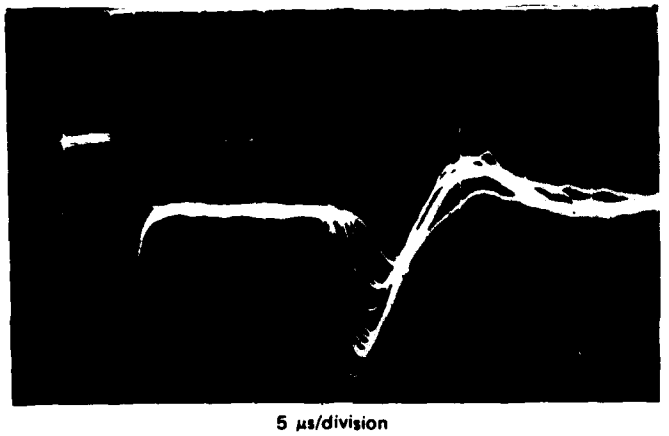

FIGURE 3 PRESSURE PULSE AT 25 torr AMBIENT PRESSURE
(100 preamplifier gain, 4-μs RF pulse, 6 discharge regions)

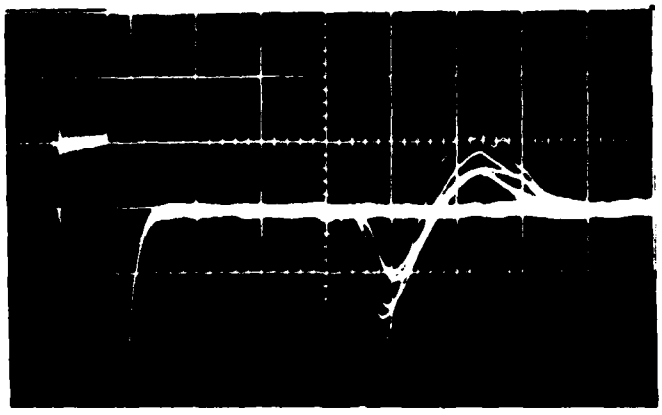

FIGURE 4 PRESSURE PULSE AT 30 torr AMBIENT PRESSURE
(100 preamplifier gain, 4-μs RF pulse, 2 discharge regions)

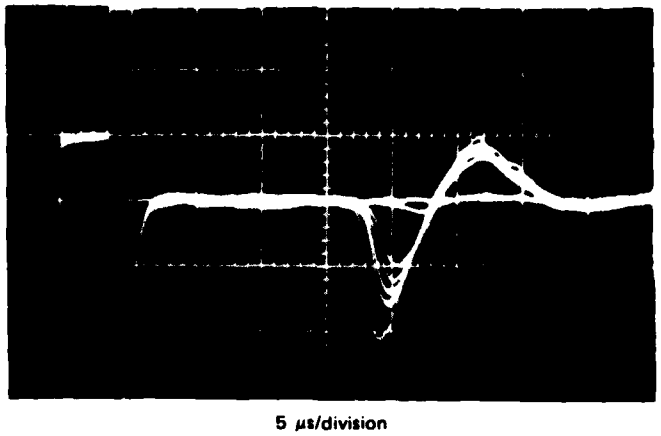

FIGURE 5 PRESSURE PULSE AT 32.5 torr AMBIENT PRESSURE
(100 preamplifier gain, 4-μs RF pulses, 10 pulses per second,
1 discharge region)

incident power was near the breakdown threshold). The variation in pressure amplitude probably corresponds to variations in energy deposited in the discharge regions, perhaps due to variations in the onset of breakdown after the beginning of the RF pulse.

Figures 2 through 5 were made at different ambient pressures. One characteristic of the traces made at ambient pressures above 25 torr is a consistent relation between the magnitude of the pressure pulse and the time of arrival of the maximum pressure, that is, the stronger the peak pressure, the sooner the peak arrives after the end of the RF pulse. At ambient pressures under 25 torr, this correlation was not observed.

Using the largest observed signal in Figure 4 as an example, the maximum pressure rise above the ambient pressure (30 torr) is:

$$60 \text{ mV} \times 0.9 \text{ torr/mV} = 54 \text{ torr} \quad .$$

Note that the pressure is approximately doubled as it is reflected off the pressure transducer and reflecting plate. This means the pressure wave emanating from the discharge had a peak overpressure of about 27 torr for this case.

Determining the temperature of the plasma (Section IV-A) requires calculating the Mach number of the pressure wave. The Mach number can be calculated directly using data from Figures 2 through 5 and the formula:

$$M = V_p/V_s = d_p/t_p V_s \quad ,$$

where

M = Mach number

V_p = Velocity of the pressure pulse

V_s = Velocity of sound under ambient conditions

d_p = Distance that the pressure pulse travels

t_p = Time that the pressure pulse takes to travel the distance d_p.

The distance from the reflecting plate to the center of the discharge region was found experimentally to be 9.7 mm, as described in Section III-A. The peak pressure is believed to occur when gas originally at that location strikes the transducer. Hence, d_p is taken as 9.7 mm. The values for t_p are determined from Figures 2 through 5, and can be found by measuring the time between the end of the discharge (or the end of the RF pulse shown in the top trace) and the peak pressure. This t_p value has some uncertainty because of heating during the beginning of the RF pulse, and because of possible flow away from the discharge before the RF pulse has ended. A calculation of the time required for the discharge to move apart significantly (half the physical width of the discharge region divided by the velocity of sound at the final temperature) indicates that the discharge stays together for about 1.6 to 1.8 μs, which is less than the discharge duration of 3.5 μs. Taking the 30 torr case as an example (Figure 4), the Mach number is 1.44 for a 27 torr overpressure.

C. Determination of Power Flux to the Breakdown Region

The adjustment of the microwave feed horn necessitated the calibration of the power flux to the discharge region. For this purpose, two power meter measurements were made, one of the maximum microwave power delivered to the feed horn, the other of the power received by a second horn mounted approximately where the lowermost discharge region formed. By comparing the second measurement with the first, we determine the attenuation in the focusing system and in the air between the feed horn and the discharge region. The plexiglass cover to the bell jar was not in place during the measurements. This cover is designed to be translucent to microwaves; had it been in place, it might have attenuated slightly the power delivered to the second horn.

For 4 μs microwave pulses, the average microwave power measured at the first horn was 119 kW, and the minimum was 114 kW. The attenuation through the focusing system and air, measured with the second collecting

horn, was 9.2 ±0.4 dB. Using the worst case (minimum power and maximum attenuation), the average power reaching the second horn was 12.4 kW. To calculate the microwave power flux actually incident upon the breakdown region, two factors must be accounted for: (1) the average power flux, determined by calculating the effective area of the collecting horn and then dividing the average power by this effective collection area, and (2) the spatial variation in electric and magnetic field strengths over the collecting horn aperture.

The collecting horn dimensions were 3 by 4.5 cm across the rectangular mouth, and 4.5 cm from any corner of the mouth to its respective corner of the rectangular waveguide. A horn of this dimension has an effective area of 10.42 cm^2.[6] Thus the average power flux incident at the discharge region is:

$$12.4 \text{ kW}/10.4 \text{ cm}^2 = 1.19 \text{ kW/cm}^2 \quad .$$

The power variation in the E-plane or the H-plane is given by:

$$P(x) = P_{max}\left(\frac{\sin^2 \alpha x}{(\alpha x)^2}\right) \quad ,$$

where

x = Transverse distance measured from the center of the collecting horn mouth.

α = 0.604 cm^{-1}, corresponding to 3 dB width of 4.6 cm (1.44 λ) .

The average power in the breakdown region due to spatial variation in one dimension only is then given by:

$$P_1 = \frac{1}{L}\int_0^L P_{max}\left(\frac{\sin \alpha x}{\alpha x}\right)^2 dx \quad , \qquad (1)$$

where L is the aperature length. Taking the first three terms of an expansion, the integral in Eq. 1 can be approximated as

$$P_1 \approx \frac{P_{max}}{L}\left(1 - \frac{\alpha^2 x^3}{9} - \frac{\alpha^4 x^5}{450}\right)\Bigg|_0^L \quad . \qquad (2)$$

Substituting the range 0 to L in Eq. 2 yields

$$P_1 \approx P_{max}\left(1 - \frac{\alpha^2 L^2}{9} - \frac{\alpha^4 L^4}{450}\right) \quad .$$

For the E-plane, L is 1.5 cm, and P_1 is 0.907 P_{max}. For the H-plane, L is 2.25 cm, and P_2 is 0.787 P_{max}. Thus, the ratio of the peak power flux to the average power flux in the discharge region is

$$\frac{P_{max}}{P_{avg}} = \frac{P_{max}}{P_1} \cdot \frac{P_{max}}{P_2} = \frac{1}{(0.907)(0.787)} = 1.40 \quad .$$

For the power flux, the maximum flux in the breakdown can be written in terms of this 1.40 factor and the average measured flux:

$$S_{max} = 1.40 \times S_{avg} = 1.40 \times 1.19 \text{ kW/cm}^2 = 1.62 \text{ kW/cm}^2$$

This result is used later (Section IV-B) to determine the absorption efficiency of the breakdown plasma.

D. Probe Measurements

To measure the density of ions and electrons in the plasma, another reflecting plate was designed to mount Langmuir probes for insertion in the lowermost, largest discharge region. The probes were constructed from irridium wire and were supported above the reflecting plate with a nonconductive ceramic tube. Several measurements were taken with different probe geometries and voltage biases.

In the first experimental probe set-up, three probes were mounted parallel to the reflecting plate and perpendicular to the E-field lines (to reduce RF coupling). The probes were 6 mil in diameter, 5 mm long, and were centered 8.0, 9.0, and 10.0 mm above the reflecting plate. The probes were biased with -12 V with respect to the reflecting plate, and probe current was measured across a 100 ohm resistor. This set-up attempted to measure the vertical ion and electron distribution through the plasma. During pulsing, the plasma tended to form around the probes, so that instead of one large plasma, often two or three separate plasmas formed. The results were deemed unreliable, and other attempts to minimize the plasma's separation in this vertical set-up were unsuccessful.

The second experimental probe set-up had three probes, each mounted 9.0 mm above the reflecting plate, with different diameters (3-, 6-, and 10-mil). The ceramic probes used in the first set-up were remade to provide a ground reference to the plasma itself, instead of relying on the reflecting plate 9.0 mm away as a ground reference. The new probes had three layers, a brass tube for ground return on the outside, a ceramic insulator as the second layer, and a irridium probe in the core. As the probe extended into the plasma, the layers were pealed away. At the plasma edge, a 2.5 mm length of brass ground return was exposed to the plasma. Then a 2.5 mm distance of ceramic insulator separated the brass from the irridium probe. Finally, a 5 mm length of probe extended beyond the ceramic insulator, so that the entire probe length was 1.0 cm. The probes were biased at -12 V with respect to the plasma, and the current through the probe was measured across a 100 ohm resistor.

As in the first setup, it was visually observed that the plasma forms quite differently in the presence of probes. With the three probes spaced 1.0 mm apart, the plasma remained whole, that is, there tended to be only one plasma. However, camera records show that the plasma moved quite significantly beyond its normal region. Figure 6 shows the oscilloscope recording of this set-up. Again, the top trace

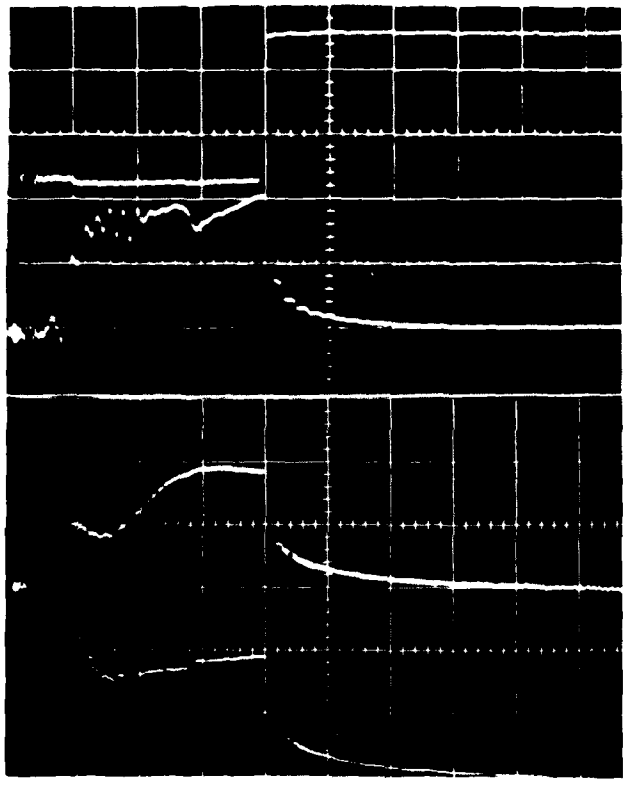

FIGURE 6 CURRENT COLLECTED BY 3-, 6-, AND 10-mil PROBES WITH -12.7 V BIAS AT 25 *torr* AMBIENT PRESSURE

shows the applied RF power in an inverted sense. The other traces show, in descending order, the 3-,6-, and 10-mil probe responses.

To provide a better ground return from the plasma using this second set-up, the 3- and 6-mil probes were then grounded and -18 V bias was applied to the 10-mil probe. The response of the 10-mil probe is shown in Figure 7. The response for several recordings was very consistent using this set-up, indicating less interference from the probes with the plasma. Unfortunately, it is impossible to determine spatial variation of the electrons and ions with a single probe. However, the densities at this single probe are discussed later in Section IV-C.

E. Optical Output of Discharges

To measure the optical output of a plasma, a photomultiplier tube (PMT) was mounted outside the protective screening of the microwave facility and pointed at the discharge region. The PMT output was monitored without amplification on an oscilloscope; Figure 8 shows a typical PMT response. As in Figures 2 through 5, two traces appear in Figure 8. The top trace shows the RF pulse in an inverted sense. The bottom trace shows the PMT response. The PMT response is uncalibrated, so the oscillogram gives only qualitative data about the optical output of a discharge region. The plasma's optical output decays rapidly and only lasts about 3 μs after the RF power pulse ends. Consequently, the photographs taken to measure plasma size represent an exposure time of pulse length plus decay time, or 11 μs per pulse. Each picture included between 10 and 100 pulses spaced 100 μs apart.

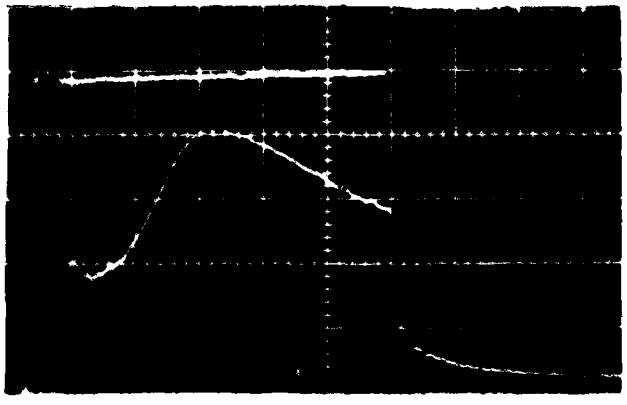

FIGURE 7 PROBE MEASUREMENT OF MICROWAVE PLASMA WITH -18 V BIAS AT 26 torr AMBIENT PRESSURE

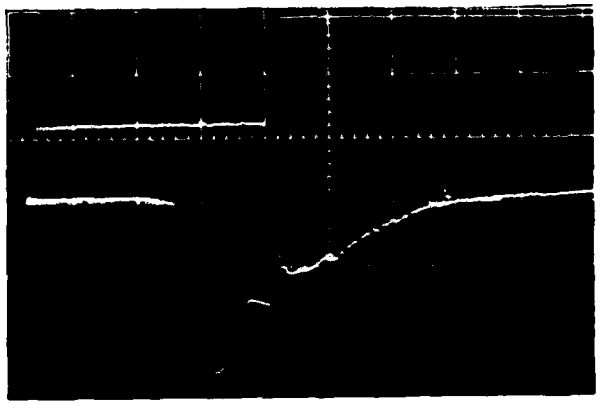

FIGURE 8 PHOTOMULTIPLIER TUBE RESPONSE AT 30 torr AMBIENT PRESSURE

IV RESULTS

A. Temperature of the Microwave Plasma

The pressure measurements described in Section III-B were made in order to calculate the temperature and the absorption efficiency of the microwave discharge (the ratio of the microwave energy absorbed by the breakdown plasma to the incident microwave energy focused on the region). The discharge temperature is calculated in this section and the absorption efficiency is calculated in Section IV-B.

The temperature of the plasma can be derived from a knowledge of energy rise in plasma. The energy absorbed is calculated by finding the Mach number of the pressure wave emanating from the breakdown, and then finding the ratio $\Delta E/E_1$, according to the one-dimensional shock theory formula given by Lin and Theofilus[4]:

$$M^2 = \frac{\gamma - 1}{2\gamma} + \frac{\gamma + 1}{2\gamma}\left(1 + \frac{\Delta E}{E_1}\right)\left[1 - \frac{\gamma - 1}{\gamma + 1}\,\frac{M^2 - 1}{M\left(1 + \frac{\Delta E}{E_1}\right)^{1/2}}\right]^{2\gamma/(\gamma - 1)} \qquad (3)$$

where

M = Mach number of shock wave

γ = 1.4 for diatomic gas (air)

ΔE = Energy increase in the plasma

E_1 = Initial thermal energy = $KT_1/(\gamma-1)$

K = Boltzmann's constant (1.38×10^{-23} joules/°K)

T_1 = Initial temperature (20°C = 293°K).

A peak Mach number of 1.44 was calculated previously (Section III-B) at 30 torr ambient pressure. However, when the overpressure is

known, it is also possible to derive the Mach number for a one-dimensional shock from the following formula:

$$M^2 = 1 + \frac{\gamma + 1}{2\gamma} \frac{\Delta P}{P} \quad , \tag{4}$$

where

ΔP = Pressure change

P_1 = Initial pressure.

Comparing calculations of the Mach number from the overpressure and from the distance traveled in a certain time checks the consistency of the experimental data. For the same maximum pressure peak in Figure 4, the Mach number derived from the above formula is 1.33, rather than the 1.44 value derived from the shock and sound speeds.

For all the discharges in Figures 3 through 5, the directly calculated Mach numbers have been plotted in Figure 9 as a function of the dimensionless quantity $\Delta P/P_1$. For comparison, Figure 9 also shows the theoretical curve corresponding to Eq. 4. Note that the directly calculated Mach numbers are greater than the theoretical Mach numbers, but that the measured and theoretical lines have about the same slope. In calculating the Mach number, we assumed that the travel distance was 9.7 mm (plasma center to pressure sensor). However, if it is assumed that the travel distance is 8.7 mm from the lower plasma edge to the sensor, then the measured and theoretical lines have similar values as well as slopes. Figure 9 shows that the pressure sensor measurements are consistent, and that they can be related to one another by dividing the pressure rises by the respective ambient pressures.

The values of $\Delta E/E_1$ derived from Eq. 3, using a specific heat of 1.40, and Mach numbers determined from both speed and overpressure measurements, are:

$$\Delta E/E_1 = 1.86 \text{ at } M = 1.33 \quad \text{(overpressure)}$$

and

$$\Delta E/E_1 = 2.62 \text{ at } M = 1.44 \quad \text{(speed)} \quad .$$

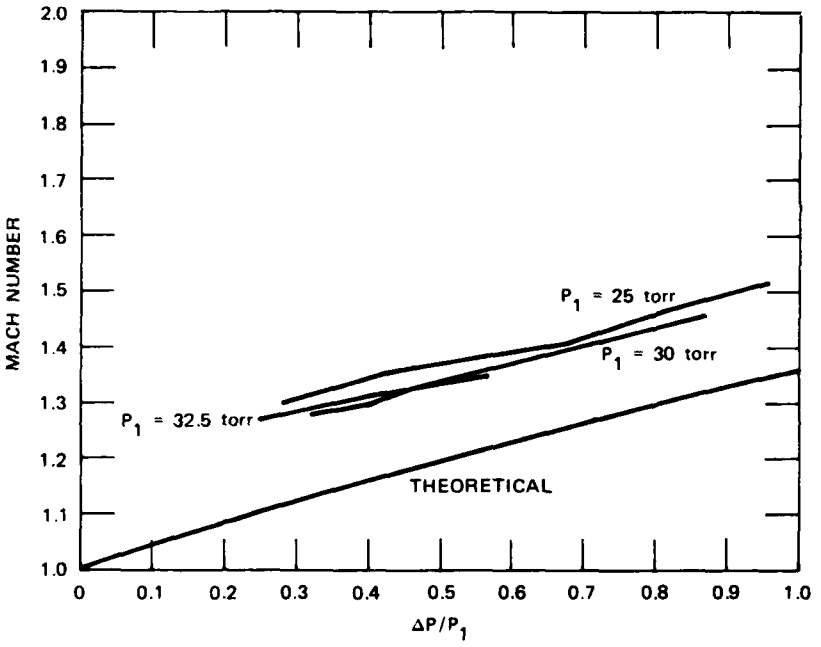

FIGURE 9 PLOT OF $\Delta P/P_1$ vs MACH NUMBER

Now the temperature of the discharge region can be derived from the absorbed energy value by the formula:

$$T = T_1 \ (1 + \Delta E/E_1) \quad .$$

For the two values of $\Delta E/E_1$ above, the plasma temperature is then 838 to 1061°K, based on 20°C ambient temperature.

B. Plasma Absorption Efficiency

From the energy rise calculated in the preceding section and the power flux measurements made in Section III-C, the absorption efficiency can now be calculated. The value of the absorption efficiency tells what percent of the microwave power incident on the discharge region is absorbed by the region. The internal energy, per molecule, is

$$E_1 = \frac{KT_1}{\gamma - 1} = 2.5 \ KT_1 \quad .$$

Hence, per molecule in the plasma region, the normalized absorbed energy for the 30 torr sample case used above is

$$\frac{\Delta E}{KT_1} = 4.65 \text{ to } 6.55 \quad .$$

This is the increase of internal energy.

The total microwave energy per unit area delivered to the plasma during discharge is derived from the experimental knowledge of the energy flux (Section III-C) and the discharge time, according to the formula

$$\Delta E_{RF} = \Delta Q = S\tau \quad ,$$

where

S = Incident power flux (1.62 kW/cm^2)

τ = Duration of the RF pulse after discharge begins (3.5×10^{-6} s).

On a per molecule basis and in terms of KT_1, Eq. 3 becomes:

$$\frac{\Delta E_{RF}}{KT_1} = \frac{ST}{L \frac{273}{T_1} \frac{P_1}{760} dKT_1} \quad , \tag{5}$$

where

L = Loschmidt's number, the number of molecules per unit volume at STP ($2.687 \times 10^{19}/cm^3$)

T_1 = Initial temperature (293°K)

P_1 = Initial pressure (30 torr)

d = Discharge thickness (0.2 cm).

The 0.2 cm thickness was measured experimentally (see Section III-A). Substituting the appropriate values into Eq. 5 yields

$$\frac{\Delta E_{RF}}{KT_1} = 7.31 \quad .$$

From this result, the energy required for ionization of the plasma could be subtracted, but that energy is very small compared to the 5 KT absorbed energy. Therefore, dividing the energy absorbed in the plasma (as deduced from the pressure and Mach number measurements) by the energy delivered, the absorption efficiency of the plasma after breakdown is between 64 and 90%. This is a high value, despite the uncertainities in our measurements. This important result signifies that little energy is reflected from the discharge region. Formation of the discharge region results in efficient coupling of incident power to the plasma, and then to the gas.

C. Electron Density

Figure 7 shows the response of a 10-mil diameter probe biased 18 V negative with respect to a 6-mil probe. Both probes are inserted in a discharge plasma, at a height of 9 mm above the reflecting plate. Positive ions are attracted to the 10-mil probe, while a return current of electrons flows into the 6-mil probe.

The RC time constant of the probe circuit is less than 100 ns, so that the time variations are followed with good accuracy. For the conditions of Figure 7, breakdown occurred about 400 ns after the RF power was turned on. Ions were immediately attracted to the probe, causing the probe current to increase rapidly to about half the eventual peak value. Over the next 2.4 μs, the probe current gradually doubled, presumably due to a gradual increase in positive ion and electron temperature and to the formation of lighter positive ions (atomic ions rather than molecular ions, breakup of ionic clusters, etc.)

At about 2.4 μs into the breakdown, the probe current began to fall. Numerous probe current oscillograms showed consistent decay after about 2.2 to 2.4 μs of probe current, despite variations in probe current onset time. Heating and expansion calculations discussed in Section III-B imply that a 2 mm thick breakdown-induced plasma will begin to expand in about 1.6 to 1.8 μs, if the plasma is fully absorbing. It is believed that such an expansion is responsible for the observed probe current decay. Taking a Mach number of 1.33, the measured expansion velocity is such that the gas moves about 0.46 mm/μs. Consequently, the positive ion current should fall to 50% of its peak value about 2.2 μs after expansion starts, assuming uniform expansion and no further ion creation or decay. The actual current is about 75% of peak value 2.2 μs after the assumed expansion begins (5.3 μs into the RF pulse). However, ionization probably continues after expansion starts.

After the RF power is turned off, the probe current drop to about one-third of its turn-off value in about 0.2 μs. This dropoff is believed to be associated with rapid cooloff of the electrons (the ion current varies as the square root of the electron temperature). Calculations indicate the electron temperature will decay according to

$$\frac{T_e(t)}{T_e(o)} = \frac{1}{(1 + t/T)^2} \quad ,$$

where

$$T = \frac{M}{2m_e \nu_c}$$

and $T = 0.19$ μs for the conditions of Figure 7. Consequently, 1 μs after RF power is turned off, 44,000°K electrons (typical of a microwave discharge) should cool to about 1150°K. Correspondingly, the ion current should drop to 16% of its turnoff value, assuming that no gas expansion occurs. In fact, that behavior is very nearly observed.

The probe currents shown in Figure 7 have been analyzed by free molecular Langmuir probe theory, and partially by continuum probe theory. Assuming an electron temperature of 44,000°K (4 eV) during the discharge, the peak probe current (when the assumed expansion starts) corresponds to a positive ion density of

$$n_+ = 5.9 \times 10^{12}/cm^3 \quad .$$

By implication, this is also the electron density. Note that this density is 4.7 times critical density ($1.09 \times 10^{12}/cm^3$ at 9.375 GHz).

The Debye length corresponding to 44,000°K and $n = 5.9 \times 10^{12}$ electrons/cm^3 is 6×10^{-4} cm. The ion mean free path for the conditions of Figure 7 is about 4×10^{-4} cm. Since the ion sheath is typically five or more Debye lengths thick (for small bias voltages), the ions will suffer eight or more collisions in moving through the ion sheath surrounding the ion collecting probe. This clearly does not correspond to free molecular theory, but it also is not strictly continuum theory, where a large number of collisions occur for an ion moving through the sheath to the probe.

At 1 μs after RF power is removed, the electrons are cooler and their Debye length is shorter. Assuming $n_e = 5.9 \times 10^{12}$ electrons/cm^3 and $T_e = 1150°K$, the Debye length is 0.96×10^{-4} cm, and only about 1.2 collisions occur while an ion moves through the sheath. This condition should be much closer to the requirements for free molecular collection. Analysis of the probe current data by the free molecular theory at 1 μs after the RF power is turned off, yields an ion density of $n_+ = 3.1 \times 10^{12}/cm^3$. We can extrapolate this value back to the time

of peak current, using the current decrease during expansion (a 0.55 factor) and an estimated attachment decay (0.82 factor).

Using these factors, the extrapolated ion density at peak current time is $6.9 \times 10^{12}/cm^3$, in good agreement with the $5.9 \times 10^{12}/cm^3$ value calculated using free molecular theory at that time.

Both of these measurements probably underestimate the actual electron density, because of collisions within the sheath. Thus the probe measurements interpreted by free molecular theory establish a lower limit of $7 \times 10^{12}/cm^3$ for the peak electron density under the conditions of Figure 7.

Continuum probe theory, which indicates electron densities greater by a factor of 1.8, is not quite applicable. Results with different size probes indicate only partial behavior in the continuum mode. We know of no validated theory in the transition region that corresponds to our case.

The product of the peak electron density and the plasma thickness gives a rough estimate of the integrated electron density. That estimate is

$$N_T = n_e \times d = 1.0 \times 10^{12} \text{ electrons/cm}^2 \quad .$$

From a theoretical basis, the integrated electron density before plasma expansion, assuming 90% power absorption, is

$$N_T = 2.30 \frac{c}{\nu} (\omega^2 + \nu^2) \frac{m\epsilon_o}{e^2} \quad .$$

At 26 torr, during the discharge, $N_T = 3.5 \times 10^{12}$. Thus, the estimated integrated electron density is about 40% of the expected theoretical value.

We conclude that the probe measurements give results in approximate agreement with theory. The probe results are probably low due to collisions that reduce the current below its free molecular value.

V SUMMARY

Several experiments have been carried out at the SRI microwave facility to determine the physical characteristics of gas discharges caused by high-power microwaves. The experiments measured the size of the discharge region, the strength of pressure waves emanating from the discharge, and the ion currents on probes in the discharge plasma for known microwave pulse durations and measured incident microwave power. From these measurements, it was possible to calculate other discharge attributes. Estimates of the plasma heating, the absorption efficiency, and the electron and ion densities of the disharge were given in the previous section. This section summarizes the measurements and the results deduced from the measurements.

The microwave power incident on the discharge region was measured as 1.62 kW/cm^2 for pulses with a 4 μs duration. These pulses create discharge regions that float about 1 cm above the reflecting plate in the vacuum chamber. The regions, which are 1.9 mm thick and about 2 cm in diameter, generally form in the antinodal spaces above the reflecting plate.

With ambient pressures in the range of 25 to 33 torr, the discharges produce shock waves that vary in strength, with the maximum somewhere between Mach 1.33 and Mach 1.44. From this pressure measurement and a knowledge of the plasma dimensions, the plasma temperature can be calculated. The plasmas were calculated to attain a maximum temperature of 838 to 1061°K. According to this calculated temperature rise in the plasma, the discharge absorbs between 64 and 90% of the measured microwave power flux incident on the discharge region. This is a remarkably high absorption efficiency, regardless of the uncertainty in the measurement.

The probe measurements show that the probes interfere significantly with discharges produced in this free-space type of discharge. This interference prevented an accurate measurement of the spatial variation of the electrons and ions in the plasma. Good measurements of the ion density were made, however, at a single point in the middle of the plasma. The peak ion densities were calculated from the ion currents collected on a probe using free molecular theory (no collisions in the sheath around the probe) and continuum theory. The value obtained for the peak ion density and, by implication, the peak electron density is $5.9 \times 10^{12}/cm^3$. Slightly higher values for peak ion and electron densities were found if the ion densities were determined after the RF pulse, when free molecular theory is applicable to interpretion of the probe data. The peak density values could then be extrapolated from the ion densities determined after the RF pulse. This technique yielded a peak ion (and electron) density of $6.9 \times 10^{12}/cm^3$. Because some collisions did occur in the probe sheath, these free molecular density estimates represent a lower bound to the actual electron and ion densities. Approximating the integrated electron density by taking the product of the peak electron density and the plasma thickness agrees reasonably with calculating the integrated density theoretically. Further measurements of the spatial variation in ion and electron density will help determine the integrated density more accurately.

REFERENCES

1. J. J. Gallagher, H. A. Ecker, M. D. Blue, and R. G. Shackelford, "Applications of Submillimeter Wave Gigawatt Sources," Final Report, Office of Naval Research Contract N00014-75-C-1011, Georgia Institute of Technology, Atlanta, Georgia (1975).

2. W. C. Taylor, W. E. Scharfman, and T. Morita, "Voltage Breakdown of Microwave Antennas," Advances in Microwaves, Vol. 17 (Academic Press, Inc., New York, 1971).

3. A. D. McDonald, Microwave Breakdown in Gases (John Wiley and Sons, New York, 1966).

4. Shao-Chi Lin and G. P. Theofilos, "Hydrodynamic Effects Produced by Pulse Microwave Discharges," The Physics of Fluids, Vol. 6, No. 10, (October 1963).

5. G. August, "Physical Constants for Microwave Discharges in Air," SRI Proposal ETU 81-69, SRI International, Menlo Park, California (May 1981).

6. Antenna Engineering Handbook, Chapter 10, H. Jasik, editor (McGraw-Hill Book Company, New York, 1961).

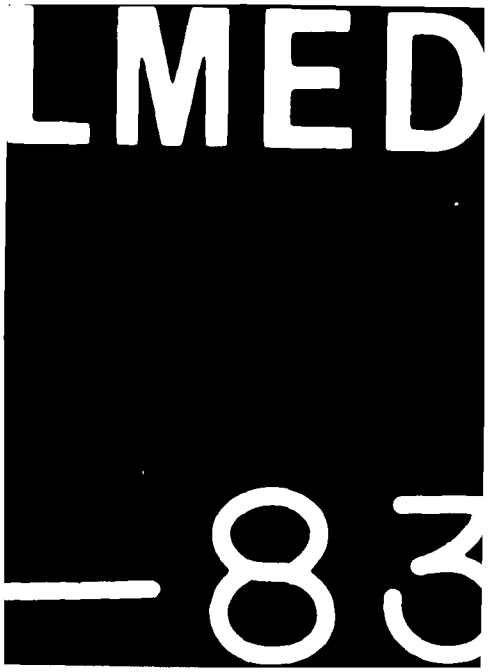
LMED
-83